



High and Equatorial Mesospheric Dynamical Response to the Minor Stratospheric Warming of 2014/15: Comparison with major SSW Events 2005/06 and 2008/09

Lynn Salome Daniel¹ · G. J. Bhagavathiammal^{1,2}

Received: 27 October 2023 / Revised: 11 March 2024 / Accepted: 8 April 2024 / Published online: 14 May 2024
© The Author(s) under exclusive licence to Korean Meteorological Society and Springer Nature B.V. 2024

Abstract

We present the high and equatorial mesospheric dynamical response to the minor stratospheric warming that occurred in 2014/15 and compared it with the major stratospheric warming events of 2005/06 and 2008/09. Meteor radar observations over Esrange (67.88°N, 21.07° E), Mohe (52.97°N, 122.53°E) and Kototabang (0.20°S, 100.32°E) have been extensively utilized in addition to ERA 5 Reanalysis datasets. Possessing the unique feature of a vortex displacement and split, the minor warming of 2014/15 was observed on 27 December 2014 followed by four subsequent temperature peaks. During the 2014/15 minor SSW, the tropical stratospheric temperature decreased, causing upwelling similar to the major SSW events 2005/06 and 2008/09. The equatorial mesospheric zonal wind in 2014/15 displayed maximum westward wind with a delay of ~ 19 days after the vortex disruption comparable to the major SSW events. Whereas, over Esrange and Mohe, the westward wind maxima occurred about the vortex disruption during all the warming events. During the minor SSW 2014/15, the ~ 16-day planetary wave is observed to be relatively stronger in the equatorial mesosphere than the high latitude mesosphere. The Eliassen Palm flux diagnostics revealed the intrusion of planetary wave energy from high latitudes to the tropical band, suggesting meridional and equatorward propagation of the planetary waves.

Keywords Stratospheric warming · Mesosphere · High-Equatorial latitude · Meteor Radar · Eliassen- Palm flux

1 Introduction

"Sudden Stratospheric Warming" (SSW) is an outstanding dynamical event in the polar winter stratosphere. The prime reason for the SSW occurrence is due to the vertically propagating planetary waves generated in the troposphere and their interaction with the mean flow (Matsuno 1971). Further, the SSW phenomenon is represented based on the evaluation of the polar vortex i.e., vortex breakdown or displacement from its polar-centric position (Andrews 1985; Kruger et al. 2005). Generally, planetary waves with wave-numbers 1 and 2 are responsible for the vortex displacement

and split processes (Charlton and Polvani 2007). The influence of SSW is not limited to the stratosphere, but it influences the higher as well as lower regions of the atmosphere, thus affecting the global circulation (Siskind et al. 2010; Wang et al. 2014; Sassi and Liu 2014; Limpasuvan et al. 2016). A major SSW is defined by the rapid rise of zonal mean polar cap temperature associated with the zonal mean zonal wind reversal at 60°N, 10 hPa, i.e., a poleward from 60 degree and above increase in temperature at 10 hPa, is observed by tens of degrees in Kelvin in association with a reversal in circulation (McInturff 1978; Butler et al. 2017). A minor SSW is defined by the rapid polar cap temperature rise at 10 hPa (Butler et al. 2015, 2017; Baldwin et al. 2021; and references therein). According to the World Meteorological Organization (McInturff 1978), an SSW is defined as a minor SSW if a significant temperature rise of at least 25 degrees in a period of about a week is observed anywhere in the winter hemisphere and at any stratospheric height. The stratospheric dynamics are becoming increasingly chaotic and irregular in their features (Das et al. 2022); hence, it is vital to understand the dynamic variability that is becoming

✉ G. J. Bhagavathiammal
selvijb@gmail.com

¹ Department of Medical Physics, Anna University, Sardar Patel Road, Chennai 600025, Tamil Nadu, India

² Centre for Climate Change and Disaster Management, Anna University, Sardar Patel Road, Chennai 600025, Tamil Nadu, India

more pronounced. A composite analysis on the stratospheric polar cap temperature and zonal wind was done by Tao et al. (2017), who highlighted that the SSWs 2003/04, 2005/06, and 2008/09 were remarkable events with strong polar cap temperature increase of 12.5 K, 7.7 K and 14.4 K respectively.

As stated by Baldwin et al. (2021), from event to event, there is a significant variability concerning the Mesosphere Lower Thermosphere (MLT) changes during SSW, showcasing the dynamics' complexity. Recently, Pedatella and Harvey (2022) found that the stratospheric polar vortex, strong and weak significantly affect the MLT region by utilizing the AURA MLS observations and WACCM Model. The impact of SSW on the mesospheric region was extensively studied by Yang et al. (2017), wherein the PW played a significant role in modulating the mesospheric dynamics. Utilizing a network of meteor radar observations covering high, mid and low latitude regions, Koushik et al. (2020a, b), investigated the MLT dynamics during the 2008/09, 2009/10 and 2011/12 SSW events. Their study signifies, that in the case of high latitudes, the mesospheric zonal wind reversal preceded the warming in the stratosphere. In mid-latitudes, the mesospheric wind showed a moderate response, compared to the high latitudes and a minimal mesospheric response was seen in the low and equatorial latitudes. In 2020, Li et al., studied the mesospheric response through a chain of meteor radar observations over China and reported that the tide-planetary wave interactions play a crucial role in affecting the MLT dynamics during SSW.

In recent decades, the influence of polar SSW on tropical latitudes has been a zestful area of research in studying the middle atmospheric dynamics. The impact of SSW on the equatorial middle atmosphere was reported for the first time by Fritz and Soules (1970) using satellite observations, followed by several authors, Mukherjee and Ramana Murty (1972), Appu (1984), Mukherjee et al. (1987), Mukherjee (1990) and Siva Kumar et al. (2003). Utilizing Rayleigh Lidar Observations over Gadanki (13.5N, 79.2 E), Sivakumar et al. (2004) observed the tropical stratospheric warming with a delay of one week after the observance of warming at the high latitudes. Further, studies suggested the cooling effect in the equatorial mesosphere during SSW (Shepherd et al. 2007) and the weakening of mesospheric winds before the onset of SSW (Hoffmann et al. 2007; Sathishkumar et al. 2009). Several authors have reported the mesospheric response to SSW events (Pant et al. 2008; Day and Mitchell 2010, Wang et al. 2014; Sassi and Liu 2014, De Wit et al. 2015; Bhagavathiammal et al. 2016; Koushik et al. 2018, Eswaraiyah et al. 2019; Qin et al. 2019, Gu et al. 2020; Koushik et al. 2022). Bhagavathiammal et al. (2016) evidenced the low latitude mesospheric dynamical response during northern (NH) and southern (SH) hemispheric SSW events, their study revealed that a more prominent evidence of planetary wave activity was found in the NH 2008/09

SSW than in the 2002 SH SW. WACCM-aided composite analysis by Limpasuvan et al. (2016) revealed Westward PW1 drag as the vital factor for the winter polar descent and stratopause recovery.

The remarkable SSW events of 2005/06 and 2008/09 and their impact were extensively investigated by several authors. Their result summarizes the tropical response to the SSW events as (i) mesospheric zonal wind and temperature variation (Hoffmann et al. 2007, Matthias et al. 2013; Chandran et al. 2014) (ii) Mesospheric PW activity (Sathishkumar and Sridharan (2009); Kuttippurath et al. 2010, 2012; Bhagavathiammal et al. 2016; Ma et al. 2017; Koushik et al. 2018; 2020a, b) (iii) convection (Kodera 2006; Sridharan and Sathishkumar 2011; Nath et al. 2013; Bal et al. 2017a, b; Bhagavathiammal 2023) (iv) variation in Brewer-Dobson Circulation (Tao et al. 2017).

Few studies have reported the minor SSW effects on the tropical middle atmospheric circulation and dynamics (Chandran et al. 2013, 2014; Medvedeva and Ratovsky 2018; Gong et al. 2019; Eswaraiyah et al. 2019, 2020). Eswaraiyah et al. (2019) reported the low latitude mesospheric response to the 2017 minor SSW, which was seen to be similar to a significant SSW event. They found weakened mesospheric winds during SSW and dominant PW activity in the mesosphere before and after SSW. Chandran et al. (2013) found evidence of secondary planetary wave generation in the high-latitude mesosphere during minor SSW. Manney et al. (2015) reported that the minor SSW of the 2014/15 winter significantly impacted the stratosphere. Table 1 lists the minor SSW events in the past decade and their vortex evaluation. Recently, Zorkaltseva et al. (2023), reported the 2013/14, 2014/15, and 2020/21 minor SSW events as unique due to the extended warming duration and the appreciable impact on the atmosphere.

Table 1 List of minor SSW events (2009–2017)

S.No	Events	Type of Vortex Disruption (Split/ Displacement)	Duration (No. of Days)
1	2009/10	Displacement	07/01/2010—07/02/2010 (31)
2	2010/11	Displacement	21/01/2011—15/02/2011 (25)
3	2011/12	Displacement	07/01/2012—21/02/2012 (45)
4	2013/14	Displacement	04/01/2014—17/02/2014 (43)
5	2014/15	Split & Displacement	27/12/2014—15/02/2015 (50)
6	2015/16	Displacement	22/01/2016—18/02/2016 (27)
7	2016/17	Displacement	20/01/2017—11/02/2017 (22)

The SSW, which occurred in 2014/15, was a long-lasting minor SSW event with a maximum duration that spanned 50 days and which had the unique characteristic of a vortex split and displacement (Manney and Lawrence 2016; Gong et al. 2019). The present study investigates the polar and equatorial mesospheric response to the minor SSW event that occurred in 2014/15, in comparison with the major SSW events of 2005/06 and 2008/09.

2 Data and Methodology

2.1 Mesospheric Winds from Meteor Radar

The present study utilizes a network of three meteor radar wind observations from Kototabang (0.2°S and 100.32°E), Indonesia, Mohe (52.97°N and 122.53°E), and Esrange Skiyet meteor radar data (67.88°N, 21.07°E) covering the high and equatorial band. The Meteor Radar at Kototabang was operated from 2002 to 2017, and is aided by the Research Institute for Sustainable Humanosphere (RISH) Kyoto University (<http://database.rish.kyoto-u.ac.jp/arch/iugonet/>). It covers an altitude range of 70–110 km at the frequency of 37.7 MHz with 12 kW output power, 13.3 ms pulse width, and 400 ms interpulse period (Batubara et al. 2011). The Esrange Skiyet Meteor Radar was operated from 2000 to 2018, covering an altitude range of 82–94 km (Mitchell 2019). It can be accessed through the website <https://catalogue.ceda.ac.uk/uuid/ba34cd217a8c49548f6fe62254b79fac>. A VHF all-sky interferometric meteor radar at Mohe (52.97°N, 122.53°E) has been in operation since 2011 (Jones et al. 1998). It can be accessed through the website <http://wdc.geophys.ac.cn/dbList.asp?dType=MetPublish>

2.2 ECMWF ERA 5 Reanalysis

The stratospheric temperature and wind components are retrieved from the fifth-generation European Centre for Medium-Range Weather Forecasts (ECMWF) ERA-5 reanalysis dataset (Hersbach et al. 2020). It is a four-dimensional dataset operated by the Copernicus Climate Change Service (C3S). The hourly temperature and wind components of spatial coverage 2.5° latitude × 2.5° longitude are utilized for the present study.

2.3 Eliassen-Palm (EP) Flux

Eliassen Palm flux and its divergence is an excellent diagnostic tool to visualize the wave-mean flow interaction, planetary wave propagation, wave breaking and many other middle atmospheric dynamical processes (Eliassen and Palm 1961; Andrews et al. 1987). Numerous authors extensively

utilized “Eliassen-Palm flux” as a tool since the 1960s (Eliassen and Palm 1961; Andrews and McIntyre 1976, 1978; Sato 1980; Edmon et al. 1980; Andrews et al. 1987; Sivakumar et al. 2004; Harada et al. 2010; Bhagavathiammal et al. 2016, 2020, 2023; Koushik et al. 2022 and many more). To achieve a realistic perception about planetary wave forcing and the interaction between background winds and planetary waves during sudden stratospheric warming, Eliassen-Palm (EP) flux vector and its divergence are computed using ECMWF ERA-5 reanalysis datasets. The EP flux vector (\vec{F}) can be represented in terms of its meridional and vertical coordinates and can also be expressed by its spherical and log pressure coordinates (Andrews et al. 1987)

$$\vec{F}^{(\phi)} = \rho_o a \cos \phi \left(\overline{u_z} \frac{v'\theta'}{\theta_z} - \overline{u'v'} \right) \quad (1)$$

$$\vec{F}^{(z)} = \rho_o a \cos \phi \left\{ [f - (a \cos \phi)^{-1} (\overline{u} \cos \phi)] \frac{v'\theta'}{\theta_z} - \overline{u'w'} \right\} \quad (2)$$

$$\nabla \cdot \vec{F} = (a \cos \phi)^{-1} \frac{\partial}{\partial \phi} \left(\vec{F}^{(\phi)} \cos \phi \right) + \frac{\partial}{\partial z} \vec{F}^{(z)} \quad (3)$$

$$D = \frac{1}{\rho_o a \cos \phi} \nabla \cdot \vec{F} \quad (4)$$

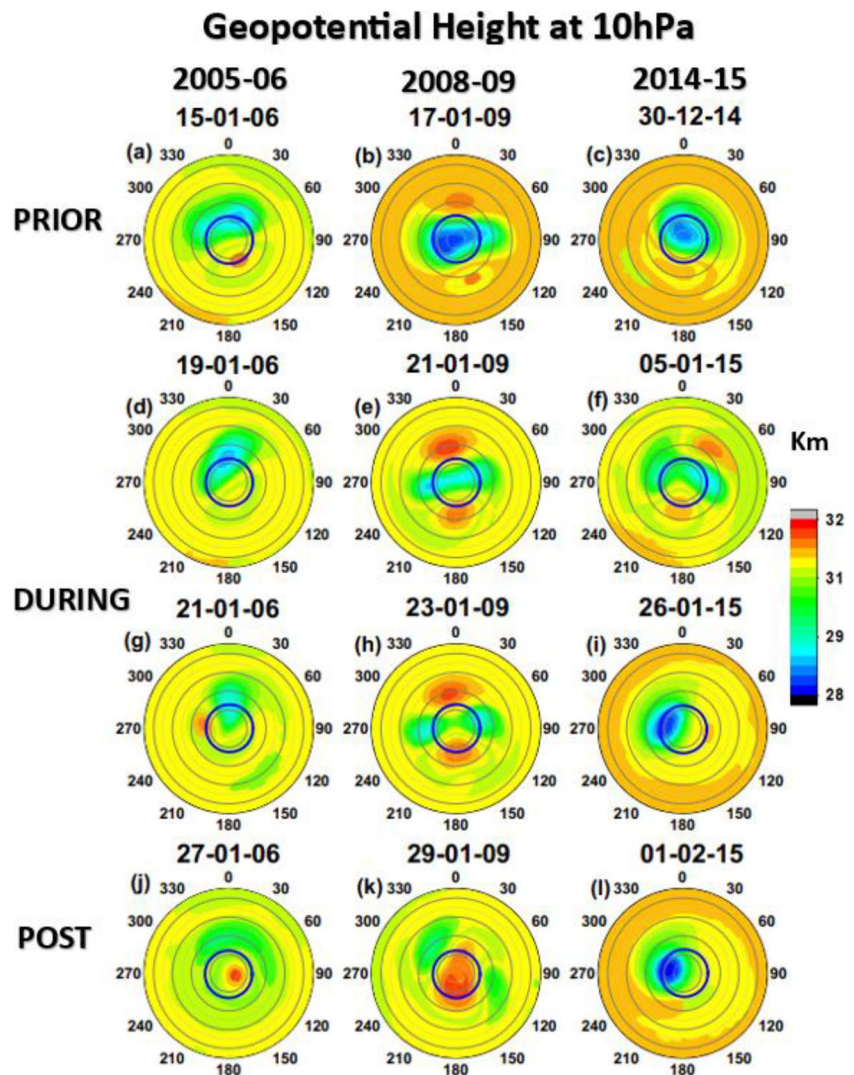
where $\phi, z, \rho_o, u, v, \theta, f$ are the meridional derivative, vertical derivative, air density, zonal component of wind, meridional component of wind, angle and Coriolis parameter respectively. The primes and overbars denote the zonal deviations and zonal averages. The vertical component of EP flux ($F(z)$) and EP flux divergence (wave driving, D) corresponds to the heat flux and the forcing of planetary waves on the mean flow respectively (Edmon et al. 1980). Enhanced heat flux represents the dominant planetary wave activity. The negative EP flux divergence represents the strong convergence of wave driving and vice versa.

3 Results and Discussions

3.1 Vortex Evolution in Major & Minor SSWs

Figure 1 describes the polar projection of geopotential height at 10 hPa for the SSW events 2005/06, 2008/09, and 2014/15. The top, middle two, and bottom panels represent the prior, during and post-conditions of the vortex evolution during SSW and the solid blue circle denotes the arctic circle. It is well-defined that the vortex displacement is merely the polar vortex shift from the pole, appearing as a ‘comma’ shape. On the other hand, vortex split is easily distinguishable as the split/break of

Fig. 1 Polar plot of geopotential height at 10 hPa for the 2005/06 (a, d, g & h), 2008/09 (b, e, h & k) & 2014/15 (c, f, i & l) SSW warmings prior, during and post the vortex disruption (displacement/split). Solid blue circle denotes the arctic circle



the vortex into two comparable sizes (O'Neill 2003). During the onset of warming, the polar eastward jet degrades and causes the polar vortex to split or displace (Butler and Gerber (2018); Hu et al. (2015); Charlton and Polvani (2007)). Figure 1a, d, g & j shows the vortex evolution during the 2005/06 SSW, and the vortex displacement that occurred on 21 January 2006 (day no. 52). The polar vortex evolution for the 2008/09 SSW is shown in Fig. 1b, e, h & k and the vortex split that occurred on 23 January 2009 (day no. 54) is shown. Figure 1c, f, i & l shows the progression of geopotential height for the minor SSW 2014/15. The appearance of a vortex split on 5 January 2015 and displacement on 26 January 2015 clearly depicts the rarity of the minor SSW 2014/15 wherein both features of vortex split and displacement are observed (Manney and Lawrence 2016). Table 1 outlines the minor SSW events and their vortex evolution.

3.2 Major & Minor SSWs

Figure 2 depicts the time-series variation of the temperature difference and zonal wind during the SSW events 2005/06, 2008/09 and 2014/15. Figures 2a, b and c represents the time-series variation of the temperature difference between 90 and 60°N at 10 hPa (solid maroon line) and 1 hPa (dashed orange line) and Figs. 2d, e and f represent the time-series variation of the zonal mean zonal wind at 60°N at 10 hPa (solid blue line) and 1 hPa (solid teal line) for the three SSW winters 2005/06, 2008/09 and 2014/15.

The horizontal purple and vertical black dashed lines represent the zero-wind line and the day on which the polar vortex displacement (split) occurred. The solid vertical maroon and black lines denote the onset and end of warming respectively. Figure 2a shows the temperature profile of the 2005/06 SSW at 1 and 10 hPa. Figure 2d shows the

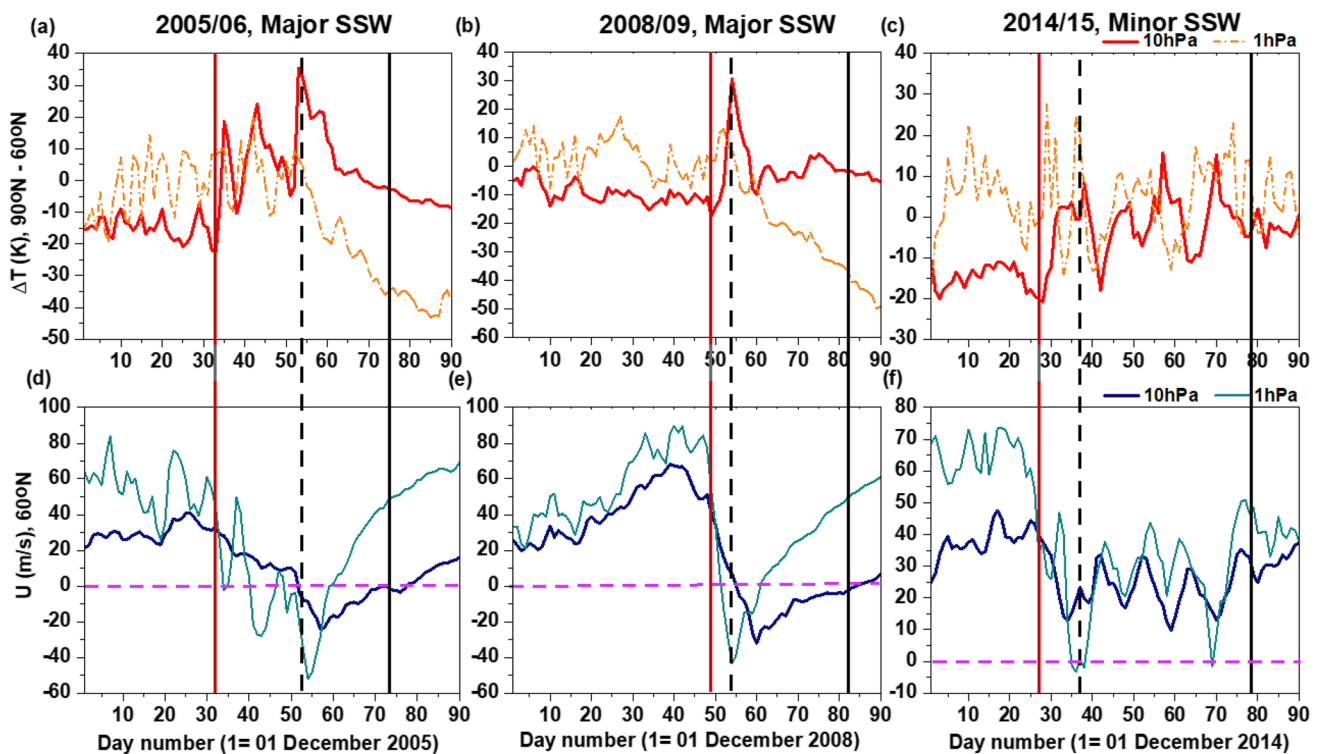


Fig. 2 Temporal variations of the polar cap temperature (90°N – 60°N) at 10 hPa & 1 hPa (**a**, **b** & **c**) and zonal wind variations at 60°N at 10 hPa & 1 hPa (**d**, **e** & **f**) for the 90 days of winter from 1 December to 28 February for the three SSWs. The vertical

solid maroon line, the vertical dashed black line and the vertical solid black line denotes the onset of warming, polar vortex disruption (displacement/split) and the end of warming respectively. The horizontal dashed purple line denotes the zero-wind line

zonal mean zonal wind profile of the 2005/06 SSW at 1 and 10 hPa. From Fig. 2a, three warming pulses were observed on 4 January 2006 (day no. 35), 11 January 2006 (day no. 42) and 21 January 2006 (day no. 52), with a temperature difference of 32 K, 38 K and 49 K from the 30-day mean temperature before the onset of warming at 10 hPa. However, the temperature profile at 1 hPa though erratic, coincides with the peak temperature at 10 hPa. In connection with the temperature rise at 10 hPa, deceleration of zonal wind from eastward to westward was observed on 20 January 2006 at the 3rd peak of warming (Fig. 2d), and reaches maximum westward velocity ~ 30 m/s on 26 January 2006 (day no. 57). The warming persisted till 17 February 2006 (day no. 79). The zonal wind at 1 hPa is associated with the temperature at 10 hPa showing three minima on 3 January, 10 January and 20 January 2006 (day no. 34, 41 and 51), while the zonal wind at 10 hPa is observed with a delay. Figure 2b & e are the same as Fig. 2a & d, but for the winter 2008/09. The onset of warming was observed on 17 January 2009 (day no. 48) at 10 hPa, it reached maximum temperature on 23 January 2009 (day no. 54) with a temperature deviant of 45 K when the vortex split was observed (as seen in Fig. 1). A spike in temperature at 1 hPa was observed prior to the temperature peak at 10 hPa (Fig. 2b). From Fig. 2e, the zonal

wind at 10 hPa is found to decelerate reaching maximum magnitude of westward wind at ~ -40 m/s on 29 January 2009 (day no. 60). At 1 hPa, wind reversal was observed one week prior on 23 January 2009 (day no. 54) as opposed to 29 January 2009 (day no. 60) at 10 hPa and it was found to be more in phase with the temperature peak at 10 hPa. Figure 2c & f elaborates on the temperature and wind profile of the 2014/15 SSW at 1 and 10 hPa. From Fig. 2f, at 10 hPa, the onset of minor SSW was observed on 27 December 2014 (day no. 27). On 5 January 2015 (day no. 36), temperature difference from the mean temperature was about 27 K, followed by successive peaks on 17 January 2015 (day no. 48), 26 January 2015 (day no. 57) and 7 February 2015 (day no. 69) with a temperature deviant of 17 K, 29 K and 29 K respectively. Tang et al. (2021) reported the rise and fall in temperature fluctuations from 27 December 2014 (day no. 27) till mid-February (day no. 77). At 1 hPa, four successive warming pulses were observed on 31 December 2014, 15 and 23 January 2015 and 3 February 2015 (day no. 31, 46, 54 and 65). In connection with the temperature variation, zonal mean zonal wind at 60°N at 10 hPa shows a decelerating trend with no wind reversal whereas in the case of 1 hPa, zonal wind at 60°N dabble near the zero-wind line at the stages of the first and fourth warming pulse with intense

deceleration but does not show prominent wind reversal. Figures 2c & f show the signatures of a minor SSW event.

3.3 Equatorial Stratosphere During Major & Minor SSW

Figure 3 describes the equatorial stratosphere during major (2005/06, 2008/09) and minor (2014/15) SSW. Figure 3a, b, and c shows the time-altitude cross-section of zonal mean zonal wind averaged over the latitude $\pm 10^\circ$ for the winters 2005/06, 2008/09, and 2014/15 respectively. The black vertical dashed line represents the date of polar vortex displacement or split and the solid vertical maroon and black lines denote the onset and end of warming respectively. In the winters 2005/06 and 2014/15, the stratosphere covering 28–43 km shows dominance of weak eastward which extends throughout the winter. However, the appearance of intense westward wind is found near the stratopause in both 2005/06 (18 December 2005 to 29 January 2006) and 2014/15 (from the beginning of December to mid-February). In addition, the downward progression of westward zonal wind is observed after the breakdown of polar vortex through displacement/split in both the winters 2005/06 and 2014/15. However, the progression is more prominent in 2014/15 minor SSW. This shows that the zonal wind evolution during the 2014/15 minor SSW displays a similar kind of signature to the major SSW 2005/06. In the case of 2008/09 winter (from Fig. 3b), the stratosphere is extensively dominated by the westward zonal wind and is found to further intensify after the vortex disruption. The low latitude middle atmospheric dynamical response to the SSW events that occurred in 1998–99, 2003–04 and 2005–06 was studied by Sathishkumar et al. (2009). They observed enhanced

westward (eastward) wind in the low latitude mesosphere (stratosphere) suggesting the effect of SSWs on tropical latitudes. Further, similar dynamical signatures were seen in the upper stratosphere and lower mesosphere whereas the middle and lower stratosphere showed similar but distinct features from the upper stratosphere and lower mesosphere after the onset of SSW (Mukhtarov et al. 2007). In 2014, Chandran et al. reported the appearance of westward wind in the equatorial region during 2008/09 warming when the QBO was dominated by the Eastward phase. Koushik et al. (2020a, b) reported the possible reasons for the acceleration in westward wind during SSW as such (i) SSW affects the equatorial stratospheric wind which allows the PW from high latitudes to propagate toward the equator and further westward wind appearance at the stratopause region (Chandran et al. 2014). (ii) the presence of inertial instabilities at the extratropical stratosphere associated with the SSW (Sassi et al. 1993).

Figure 3d, e, and f represent the time-altitude cross section of zonal mean temperature averaged over the latitude band $\pm 10^\circ$ for the winters 2005/06, 2008/09 and 2014/15 respectively. All three SSW events show a strong upwelling (cooling) in the equatorial stratospheric temperature in connection to the polar cap temperature rise and vortex disruption. It is found that prominent upwelling is seen around 21 January 2006 (day no. 52), 23 January 2009 (day no. 54), and 5 January 2015 (day no. 36) for the SSW events 2005/06, 2008/09 and 2014/15 respectively. Tao et al. (2017) investigated the tropical upwelling response to the SSW and non-SSW events along with their QBO phases and found that in most cases increased upwelling was recorded as a response to SSWs through the Brewer Dobson circulation. At 10 hPa during the 2008/09 SSW, the temperature was

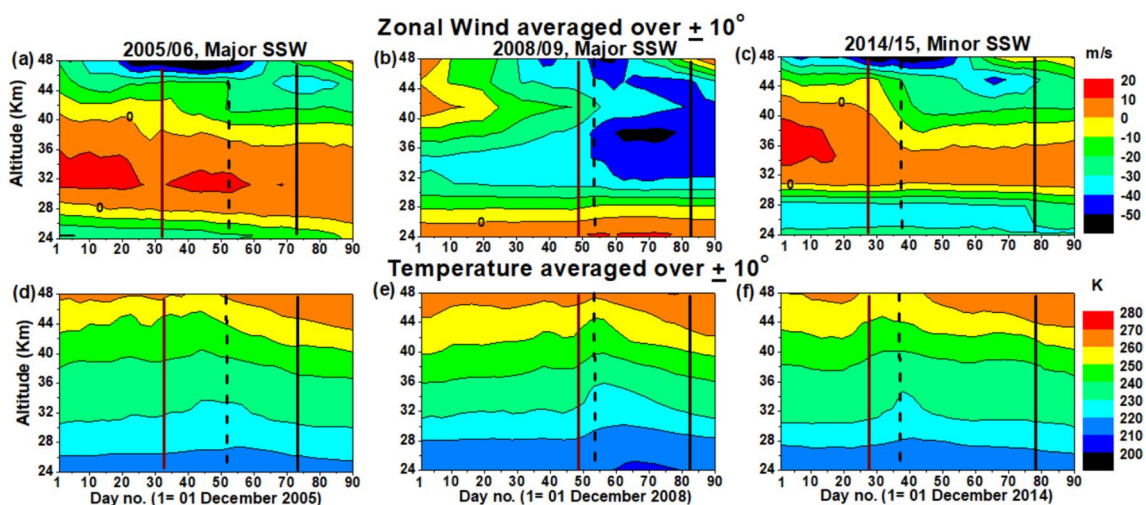


Fig. 3 Time-altitude cross-section of the stratospheric zonal wind (a, b & c) and stratospheric temperature (d, e & f) averaged over the equator. The vertical solid maroon line, the vertical dashed black line

and the vertical solid black line denotes the onset of warming, polar vortex disruption (displacement/split) and the end of warming respectively

seen to peak on 23 January 2009 (day no. 54). In association with the rise in temperature at the polar regions, an evident drop in temperature was observed over the tropical regions. The upwelling (150–100 hPa) was suggested to be caused due to the strong wave activity observed over the polar regions and its meridional propagation toward the equator (Yoshida & Yamazaki 2011).

3.4 Status of Polar and Equatorial Mesosphere during major & minor SSW

The mesosphere is an active dynamical region that greatly responds to the dynamical processes in the lower atmosphere. Figure 4 depicts the polar and equatorial mesosphere for the three winters of 2005/06, 2008/09, and 2014/15. Figure 4a-d represents the time-altitude cross-section of daily mesospheric zonal wind over Esrance (a, b) and Kototabang (c, d) for the winters 2005/06 and 2008/09 respectively. The black dashed line indicates the date on which the polar vortex disruption (displacement or

split) occurs and the solid vertical maroon and black lines denote the onset and end of warming respectively.

During the 2005/06 winter (from Fig. 4a), it is found that a large eastward (~ 60 m/s) wind dominates the polar mesospheric zonal wind except during 20 December 2005 (day no. 20) and 21 January 2006 (day no. 52) wherein the presence of westward wind of ~ -30 m/s in the lower altitudes over Esrance is observed for a short time prior to and about the occurrence of vortex displacement. The equatorial mesospheric zonal wind over Kototabang (Fig. 4c) is dominated by weak eastward and weak westward conditions, whereas after the vortex disruption, strong westward zonal wind is observed during the 2005/06 winter.

Likewise, in the case of the 2008/09 winter (Fig. 4b), the eastward wind is seen to dominate the polar mesosphere over Esrance before and after vortex split; but about the time of vortex split, westward wind reaches a maximum of -36 m/s on 24 January 2009 (day no. 55). Reverse to the high latitude mesosphere, the equatorial mesospheric zonal wind over Kototabang (Fig. 4d) showcases

MESOSPHERIC ZONAL WIND OVER ESRANGE (67.88°N, 21.07°E) & KOTOTABANG (0.2°S, 100.32°E)

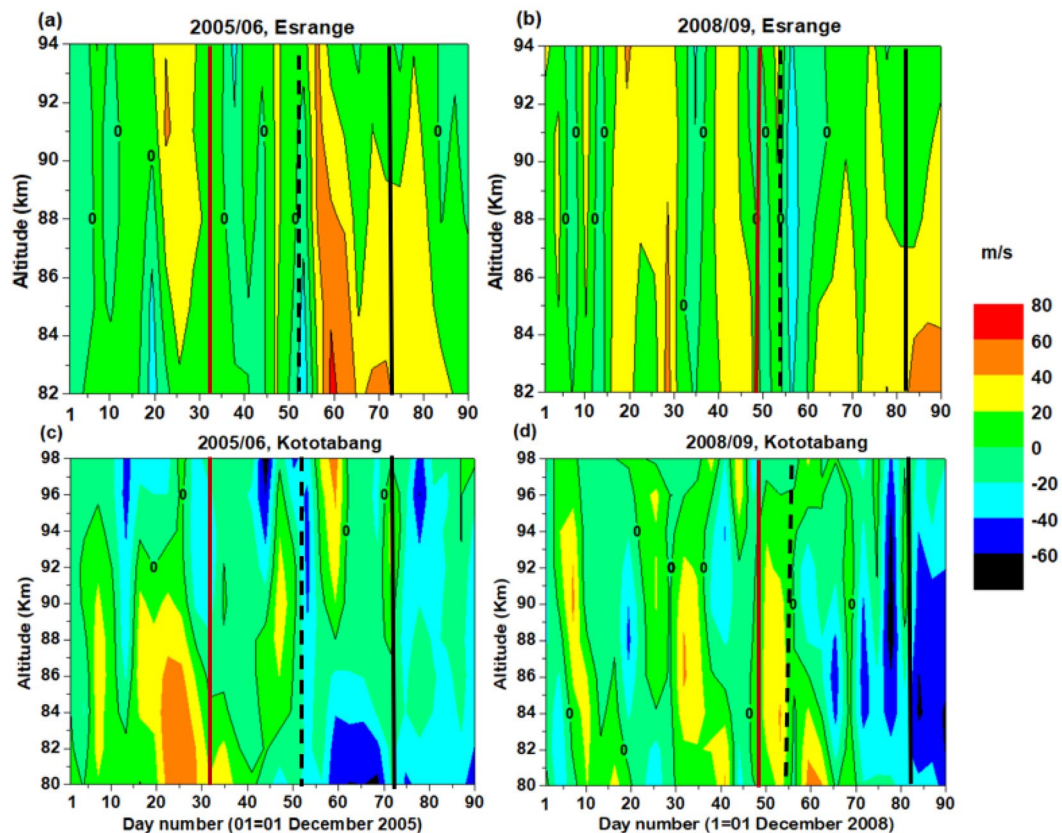


Fig. 4 Time-altitude cross-section of daily mesospheric zonal wind over Esrance (67.88° N, 21.07° E) (a, b) & Kototabang (0.20°S, 100.32°E) (c, d) during the 2005/06 & 2008/09 major warmings. The

vertical solid maroon line, the vertical dashed black line and the vertical solid black line denotes the onset of warming, polar vortex disruption (displacement/split) and the end of warming respectively

the appearance of weak eastward until vortex disruption after which it is dominated by the westward zonal wind.

The mesospheric zonal wind over Kototabang reaches westward maxima ~10–20 days after the vortex disruption for the 2005/06 and 2008/09 SSWs. The mesospheric zonal wind over Esrangle showcase similar behaviour for the winters 2005/06 and 2008/09. In the case of the equatorial mesosphere, the zonal wind continues to be westward after the reversal till the end the winter.

Table 2 describes the observed mesospheric wind characteristics over Esrangle & Kototabang during the 2005/06, 2008/09 & 2014/15 SSWs. Table 2 encapsulates the central date (date on which vortex disrupts), mean zonal wind during vortex disruption and maximum westward wind observed at MLT. In the mesosphere, the magnitude of the peak westward wind over Kototabang was found to be nearly twice the magnitude of the peak westward wind over Esrangle/Mohe. The peak westward over Kototabang appears with a delay of nearly ~10–20 days after the vortex disruption, whereas over Esrangle/Mohe, the peak westward was seen to appear around the vortex disruption.

The SSW events 2005/06 and 2008/09 have been extensively studied by several authors. Hoffmann et al. (2007), reported a short reversal of the mesospheric zonal wind over Andenes (69°N, 16°E) and Juliusruh/ Kühlungsborn (54°N, 12–13°E) followed by a band of intensified eastward winds. This result agrees with Hoffmann et al. (2007) wherein a short eastward to westward reversal followed by the persistence of strong eastward wind at high latitude mesosphere was observed. In the case of the equatorial mesosphere, the zonal wind reversal occurred before the warming and peak westward appeared with a delay of ~10–20 days after vortex disruption, in agreement with Sathishkumar et al. (2009).

Figure 5a b&c, describes the polar and equatorial mesospheric zonal wind during the minor 2014/15 SSW over Esrangle, Mohe, and Kototabang respectively. Due to the sparse data availability over Esrangle during the 2014/15 minor warming, we take Mohe into consideration. During minor SSW 2014/15, the mesospheric zonal wind observation over Esrangle and Mohe shows intense and strong eastward wind (40–80 m/s) with a sharp wind reversal around the vortex disruption. Whereas, in the equatorial mesosphere (Fig. 5c), we see the appearance of an intense westward wind ~10 days after the vortex split. The peak westward maxima of magnitude -70 m/s is observed about 10 days after the vortex disruption on 24 January 2015 (day no. 55), this result is in agreement with Ma et al. (2017), wherein the westward wind with a peak magnitude of -75 m/s was observed strongest over low latitude Sanya after the onset of SSW in comparison to the weak signatures over high latitude Mohe.

Figures 6 and 7 describes the wavelet power spectrum of planetary waves in the mesospheric altitudes for the winters 2005/06, 2008/09, and 2014/15. The Morlet wavelet technique is an efficient method to visualize the planetary waves in the mesosphere and their temporal evaluation (Torrence and Gilbert 1998; Rao 2002; Pancheva and Mukhtarov 2000, Chen and Chu 2017). The black dashed line indicates the date on which the polar vortex disrupts (displacement/split) and the solid vertical maroon and purple lines denote the onset and end of warming respectively. The white contour represents the regions of greater than 95% confidence of the planetary wave oscillations observed. For better understanding, the x-axis is shown by lead-lag representation in steps of 10 days with reference to the vortex disruption. The upper panel of Fig. 6 shows the wavelet power spectrum of hourly zonal mesospheric wind at 88 km over Esrangle

Table 2 Observed characteristics of minor SSW (2014/15) in comparison with major SSWs (2005/06 & 2008/09)

S.no	SSW	Year	Station	Central date*	Observed maximum westward wind (Date of occurrence) at MLT	Delay (No. of Days)	Mean zonal wind at MLT during vortex disruption	
1	Major	2005/06	Esrangle	21 Jan 2006	-35 m/s (21 Jan 2006)	0	14.2 m/s	
			Kototabang					
	2008/09	Esrangle	23 Jan 2009	-68 m/s (31 Jan 2006)	10	-6 m/s		
		Kototabang						
2	Minor	2014/15	Esrangle	05 Jan 2015	-32 m/s (03 Jan 2015)	-2	10.1 m/s	
			Mohe					
			Kototabang					
					-36 m/s (24 Jan 2009)	1	3.2 m/s	
					-77 m/s (15 Feb 2009)	23	-32.4 m/s	
					-37 m/s (04 Jan 2015)	-1	17.4 m/s	
					-70 m/s (24 Jan 2015)	19	-6 m/s	

*The Central date is the day the polar vortex disrupts (displaces/ splits) at 10 hPa. It is denoted by the dashed line in Figs. 2, 3, 4, 5, 6 and 7

MESOSPHERIC ZONAL WIND OVER ESRANGE (67.88°N, 21.07°E), MOHE (52.97°N, 122.53°E) & KOTOTABANG (0.2°S, 100.32°E)

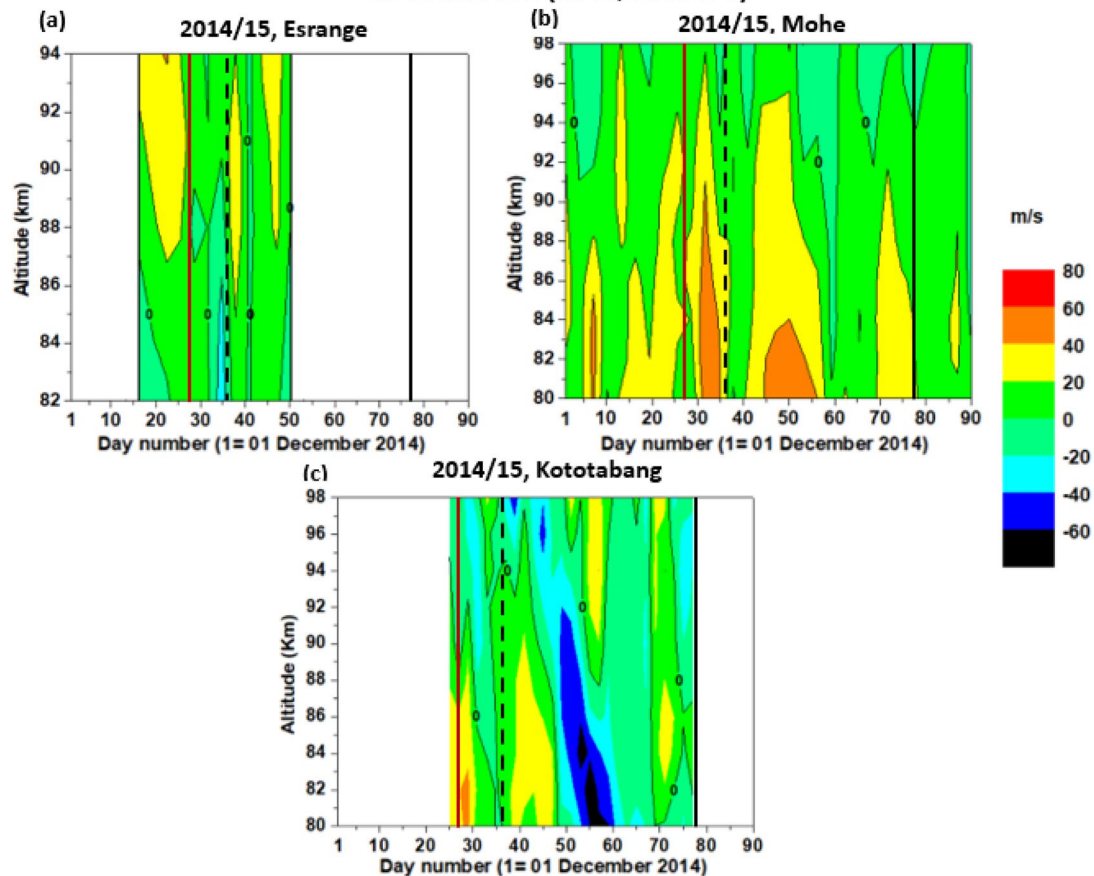


Fig. 5 Time-altitude cross-section of daily mesospheric zonal wind over Esrange (67.88° N, 21.07° E) (a), Mohe (52.97° N, 122.53° E) (b) & Kototabang (0.20°S, 100.32°E) (c) during the 2014/15 minor warming. The vertical solid maroon line, the vertical dashed black

line and the vertical solid black line denotes the onset of warming, polar vortex disruption (displacement/split) and the end of warming respectively

for the winters 2005/06 and 2008/09. From Fig. 6a, we can see the appearance of the Q8DW ($\sim 20 \text{ m}^2\text{s}^{-2}$) around 12 December 2005 and the Q10DW ($\sim 40 \text{ m}^2\text{s}^{-2}$) strongly at the time when the polar vortex disrupts. Figure 6b presents the wavelet power spectrum for the winter of 2008/09 over Esrange. It shows the presence of a quasi-16-day oscillation prior to the vortex disruption. In addition, a quasi-5-day wave is observed at the beginning of December. An intense quasi-6.5-day wave is observed just a few days before the vortex split. The bottom panels (Fig. 6c and d) describe the planetary wave oscillation over Kototabang for the winters 2005/06 and 2008/09. From Fig. 6c, we can infer the vigorous planetary wave activity at the beginning of the 2005/06 winter. Combined Planetary wave signatures of quasi-10-day and quasi-16-day waves of maximum power $\sim 37 \text{ m}^2\text{s}^{-2}$ are noted in December. A similar PW feature is observed in the polar latitude and is found at the time the polar vortex disrupts. In the case of 2008/09, from Fig. 6d, the presence

of a quasi-16-day wave with a maximum power of $50 \text{ m}^2\text{s}^{-2}$ is found after the polar vortex disrupts. In addition, a strong quasi-6.5-day wave was observed in February.

Matthias et al. (2013) reported the appearance of quasi-6, 10, and 16 day waves during major warmings in 2005/06 and 2008/09 using MLT geopotential data. The amplitude of the quasi-16-day wave was found to be weaker in comparison to the quasi-6 and 10-day waves. Koushik et al. (2020a, b) reported 6–10-day waves over low and equatorial latitudes Thumba and Kototabang that were seen after the central date with a marked delay in comparison with the mid-latitude station “Sorocco”. This study agrees with the above study on the 2005/06 and 2008/09 SSW, wherein during SSW planetary wave oscillations Q6DW, Q10DW and Q16DW in geopotential data were reported, our work validates the periodicities in the mesospheric zonal wind. Similar to what Koushik et al. 2020a, b reported, the 6–10 day waves are observed after the vortex disruption.

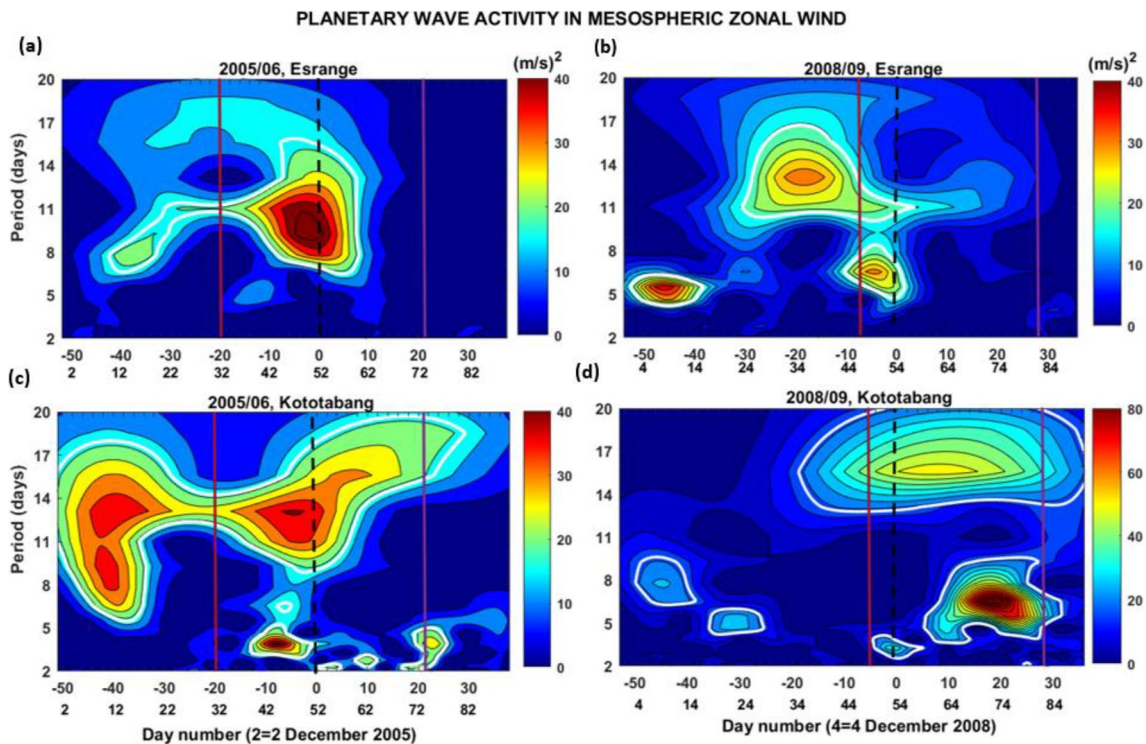


Fig. 6 Wavelet power spectrum of zonal wind at 88 km from the polar and equatorial radar site at Esrange (67.88° N, 21.07° E) (a, b) & Kototabang (0.20°S, 100.32°E) (c, d) during the 2005/06 & 2008/09 major warmings. The vertical solid maroon line, the vertical

dashed black line and the vertical solid purple line denotes the onset of warming, polar vortex disruption (displacement/split) and the end of warming respectively. The white contour represents the region of greater than 95% confidence

Figure 7a, b, c presents the wavelet power spectrum of mesospheric zonal wind at 88 km over Esrange, Mohe, and Kototabang for the winter 2014/15. From Fig. 7a, a weak quasi-16-day wave appeared prior to the vortex disruption. In addition, a quasi-5-day wave is strongly observed after the vortex disruption. Strengthening the results, mesospheric zonal wind observations over Mohe, show similar features with increased power. Figure 7c shows the wavelet power spectrum of mesospheric zonal wind at 88 km over Kototabang for the winter 2014/15. An intense quasi-16-day wave appears just prior to the vortex disruption and continues throughout the warming with maximum power of $100 \text{ m}^2\text{s}^{-2}$. Further, a quasi-8-day wave is weakly observed prior to the vortex disruption. From Fig. 7a-c, the quasi 16-day planetary wave features are found to appear strongly in all three stations Esrange, Mohe, and Kototabang with maximum intensity at equatorial latitudes and weaker amplitudes over the polar regions.

3.5 Wave Flux Over High and Equatorial Latitudes

The altitude-time cross-section of wave flux averaged over high $60^\circ\text{-}80^\circ$ (top panels – Fig. 8a, b & c) and tropical latitudes $0^\circ\text{-}30^\circ$ (bottom panels – Fig. 8d, e & f) for the winters 2005/06, 2008/09 and 2014/15 are shown in Fig. 8. The dashed white line indicates the date on which the polar vortex

disrupts and the solid vertical maroon and purple lines denote the onset and end of warming respectively. Eliassen Palm (E-P) flux is widely used as a diagnostic tool to visualize the planetary wave propagation in the middle atmosphere. Figure 8 shows the time-height cross-section of the vertical component of E-P flux, $F(z)$. Recently, Bhagavathiammal (2023) reported the equatorward propagation of planetary waves from the extra-tropical region to the tropics during mid-winter stratospheric warming events 2003/04, 2005/06, 2008/09, 2012/13 and 2018/19. Figure 8a shows persistent downward propagating wave flux with a maximum intensity of $4 \times 10^5 \text{ Kgs}^{-2}$ from the start of winter to mid-January. Specifically, three-wave flux on January 3, 9 and 20 2006 (day no. 34, 40 and 51) propagated meridionally as well as downward and reached the lower stratosphere which is seen in the tropical band with a reduced intensity $\sim 6 \times 10^3 \text{ Kgs}^{-2}$ (Fig. 8d).

Figure 8b & e represent the vertical component of heat flux $F(z)$ for the winter 2008/09 averaged over the high and the low latitude band respectively. An intense wave flux is observed around 20 January 2009 (day no. 51) at the time of vortex split with an intensity of $\sim 3.5 \times 10^5 \text{ Kgs}^{-2}$ over the high latitude band from Fig. 8b. Signatures of this wave flux are found to propagate and reach the tropical band as well as the lower stratosphere ($\sim 29 \text{ km}$) with a delay of about 7 days with intensity $\sim 6 \times 10^3 \text{ Kgs}^{-2}$.

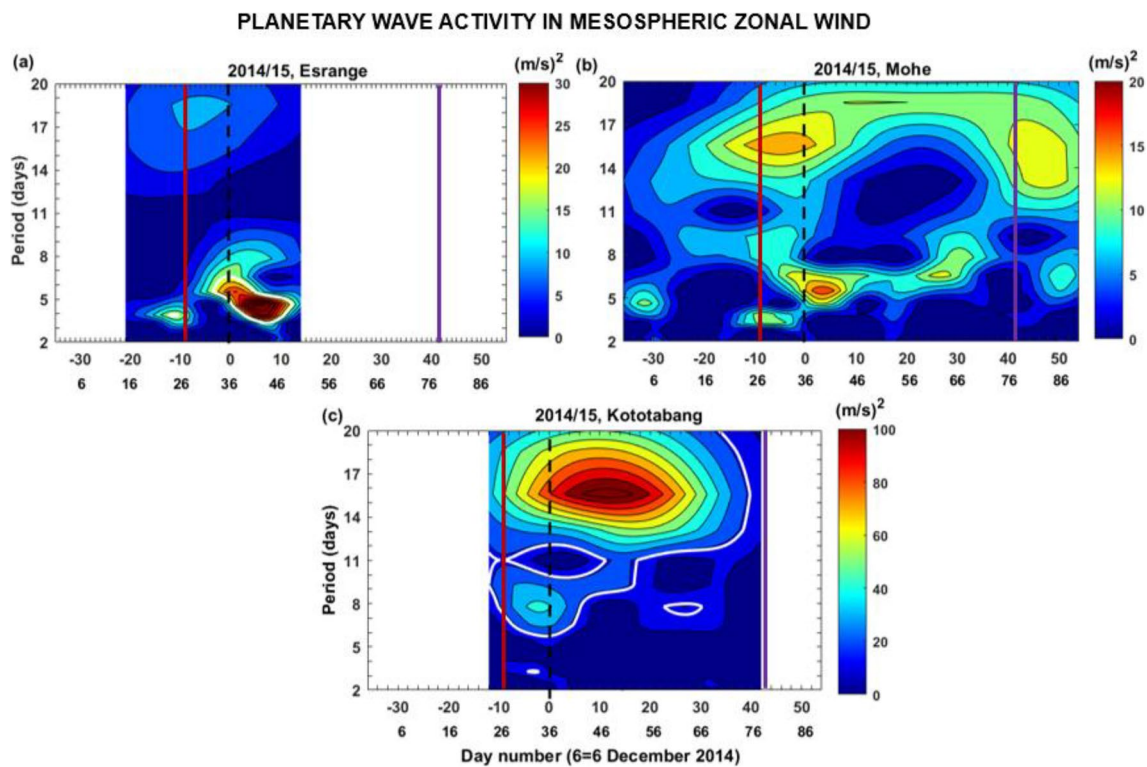


Fig. 7 Wavelet power spectrum of zonal wind at 88 km from the polar and equatorial radar site at Esrange (67.88° N, 21.07° E) (a), Mohe (52.97° N, 122.53° E) (b) & Kototabang (0.20° S, 100.32° E) (c) during the 2014/15 minor warming. The vertical solid maroon

line, the vertical dashed black line and the vertical solid purple line denotes the onset of warming, polar vortex disruption (displacement/split) and the end of warming respectively. The white contour represents the region of greater than 95% confidence

Figure 8c & f represent the vertical component of E-P flux $F(z)$ for the winter of 2014/15 averaged over high (60–80°N) and tropical (0–30°N) latitude bands respectively. An intense wave flux around 28 December 2014 (day no. 28) and 02 February 2015 (day no. 64) propagates downward and reaches up to the lower stratosphere (~24 km). In addition, a weak wave flux appeared around 19 January 2015 (day no. 50) confined to the upper stratosphere. Signatures of the 1st wave flux reached the tropical band with a delay of ten days with maximum intensity $\sim 10 \times 10^3 \text{ Kg s}^{-2}$. Furthermore, the 2nd wave flux observed around 2 February 2015 (day no. 64) propagated downward, latitudinally and reached up to the tropical middle stratosphere with the intensity of $\sim 6 \times 10^3 \text{ Kg s}^{-2}$. In comparison with 2005/06 and 2008/09, the minor SSW that occurred in 2014/15 shows the appearance of wave flux dominantly in both high and tropical latitudes. The downward and equatorward propagation of planetary waves is evident not only in the major stratospheric warmings but also in the minor stratospheric warming of 2014/15. The penetration of wave flux is more prominent in vortex split events (2008/09 and 2014/15) than vortex displacement (2005/06). Bal et al. (2017a, b) carried out a composite analysis of the warming events from 1979 – 2013 using ERA-Interim and reported that the EP flux and divergence for vortex split events in

comparison with other warmings persist longer and give a more pronounced negative divergence. Bhagavathiammal et al. (2016) reported the downward progression and reach of wave flux from extra-tropics to the tropical band with a delay of about 7 days for the winter 2008/09.

3.6 Wave Driving Behavior in Major & Minor SSWs

Wave driving is the key factor that reveals the influence of planetary wave forcing on the background mean flow. Planetary wave forcing on the mean flow is defined as the EP flux divergence (Edmon et al. 1980). Figure 9 depicts the latitude-time representation of the EP flux divergence at 10 hPa for the winters 2005/06, 2008/09, and 2014/15. The black dashed line denotes the date on which the polar vortex disrupts (displacement/split) and the solid vertical maroon and black lines denotes the onset and end of warming respectively. The arrows indicate EP flux vectors at 10 hPa and the arrowheads show the direction of propagation. The negative EP flux divergence indicates the piling up of wave activity. Figure 9a represents the latitude-time variation of the wave driving and EP flux vectors at 10 hPa during the 2005/06 major SSW. The strong convergence of wave driving is observed throughout December–January, this confirms

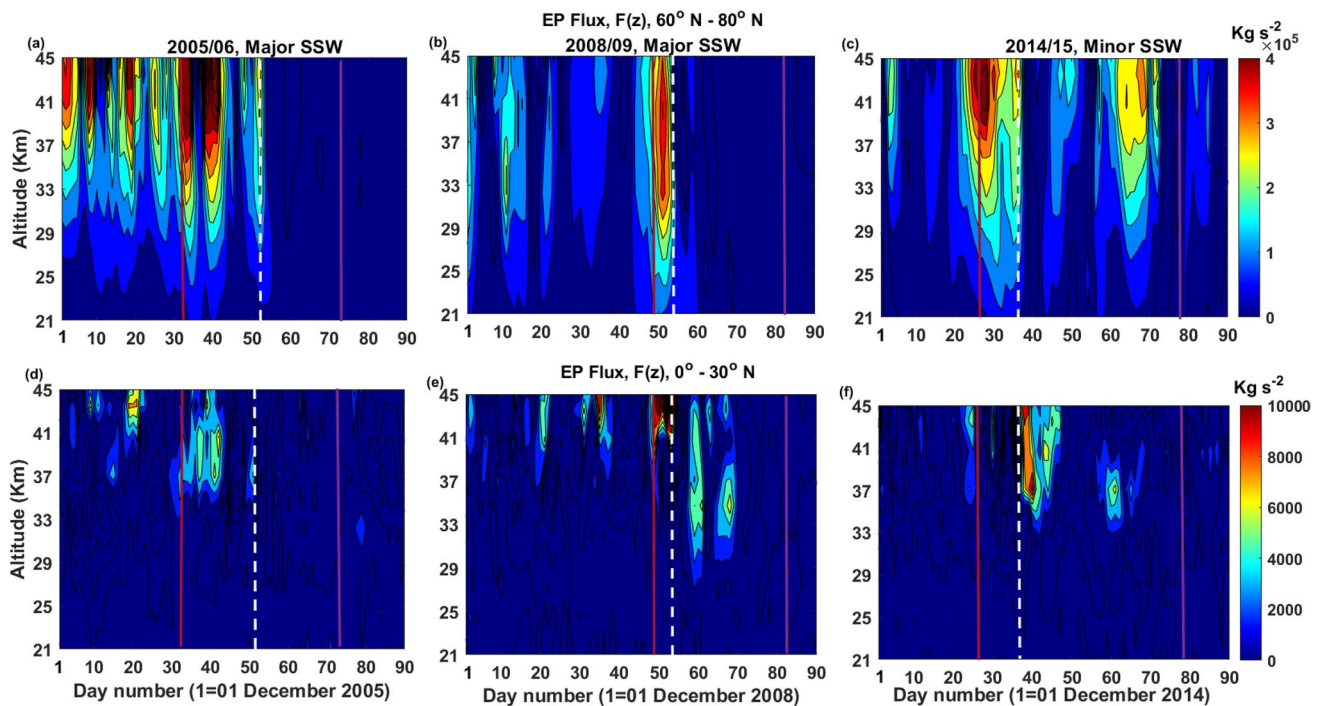


Fig. 8 Eliassen-Palm Flux, $F(z)$ averaged over the high latitude band (60° – 80° N) and low latitude band (0° – 30° N) during the 2005/06 (a, d), 2008/09 major warmings (b, d) & 2014/15 minor warming (c, f).

The vertical solid maroon line, the vertical dashed white line and the vertical solid purple line denotes the onset of warming, polar vortex disruption (displacement/split) and the end of warming respectively

again the observed from the vertical component of EP flux (Fig. 8), indicating more planetary wave activity. After the major warming, no such convergence of wave activity is seen. The vectors are tilted and the propagation towards the lower latitudes is shown around the time of vortex disruption (black dashed line). Around 15 January 2006 (day no. 46), negative convergence of wave forcing propagates downward and reaches up to the low ($\sim 10^{\circ}$ N) latitudes.

Figure 9b is the same as Fig. 9a but for the winter 2008/09. Consistent patches of convergence of Wave driving are found throughout the month of December 2008–January 2009. Compared to the 2005/06 SSW, the EP flux vectors are seen to be more evident in its propagation at the onset of warming and at the time of vortex split. Intensified convergence of EP Flux divergence is observed around the polar vortex split in mid-January 2009. This rapid convergence observed during the vortex split around 22–30 January 2009 (day no. 53–61) represents the enhanced planetary wave activity which in turn propagates downward and reaches up to the lower latitudes ($\sim 7^{\circ}$ N). In association with this, strong quasi-16-day and 6.5-day were observed with little delay in the equatorial mesosphere over Kototabang (can be found in Fig. 6d).

Figure 9c is the same as Fig. 9a and b, but for the winter 2014/15. Strong features of alternating convergence and divergence of wave forcing is observed throughout the winter. During the onset of warming, we see that the vectors

begin to tilt equatorward towards the lower latitudes and propagation is more evident about the time of vortex split. Around 9 January 2015 (day no. 40), when the vortex split occurs, Convergence of wave forcing (negative EP flux divergence) from high latitudes propagate downward and reaches up to much lower latitudes ($\sim 3^{\circ}$ N). In association with this extratropical planetary wave forcing, the wavelet power spectrum shows evidence of strong quasi-16-day wave features in Kototabang (Fig. 7). As we infer from Fig. 9, an EP flux visualizes the intrusion of planetary wave energy from high latitudes to the equatorial band around the time the vortex disrupts (displacement/split).

The minor stratospheric warming effect on the tropical atmosphere is a current topic of research. Manney et al. (2015) examined the stratospheric temperature and trace gas transport during minor stratospheric warming 2014/15 and their study revealed that the dynamical effects seemed to be as similar to that of a major stratospheric warming. Eswarajah et al. (2019, 2020) studied the low latitude mesospheric response to the 2017 minor stratospheric warming using meteor radar observations over Fuke (19.5° N, 109.1° E) and they found dominance of planetary waves of periods 20–28, 14–16 and 2–12 day before and after the stratospheric warming. Meteor radar observations at Tirupati (13.63° N, 79.4° E) showed a strong weakening of mesospheric zonal wind with temporal variations during

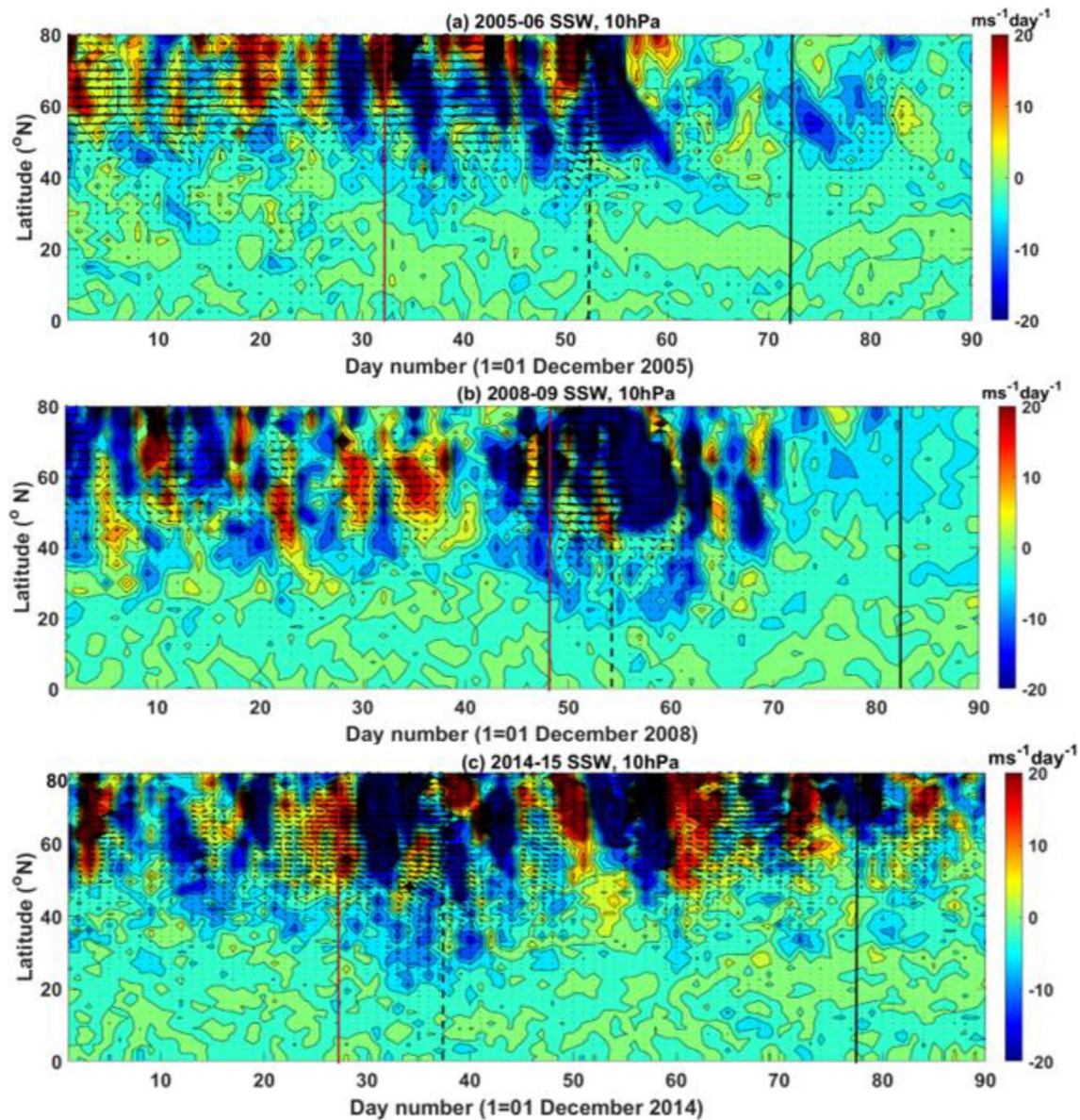


Fig. 9 Latitude-Time cross section of the wave driving and EP flux vectors at 10 hPa during the 2005/06 (a), 2008/09 (b) & 2014/15 (c) SSW warmings. The vertical solid maroon line, the vertical dashed black line and the vertical solid black line denotes the onset of warm-

ing, polar vortex disruption (displacement/split) and the end of warming respectively. The arrow heads denote the direction of EP flux vector propagation

SSW. Recently, Li et al. (2023) classified a new approach for sudden stratospheric warming and suggested that the 2014/15 minor warming was considered to be a major warming.

4 Conclusion

The present work describes the high and equatorial mesospheric dynamical response to the minor stratospheric warming that occurred in 2014/15 in comparison with the

major SSW events of 2005/06 and 2008/09. This study attempts to provide an in-depth view on the minor SSW effects of the high and equatorial mesosphere in comparison to the major SSWs. The objective was mainly executed with the help of Meteor radar observations over Esrang (67.88°N, 21.07°E), Mohe (52.97°N, 122.53°E) and Kototabang (0.20°S, 100.32°E). The unique feature of the minor stratospheric warming that occurred in 2014/15 is that it is long lasting and displays both vortex displacement and split characteristics. The onset of minor warming in 2014/15 was observed on 27 December 2014 followed by four subsequent

temperature peaks, similar to the major warming in 2005/06. Tropical upwelling is an induced process that occurs in the tropical stratosphere during major stratospheric warming. However, the minor stratospheric warming in 2014/15 also shows the signatures of tropical upwelling and temperature decrease at the time of vortex disruption, comparable with the 2005/06 and 2008/09 SSWs. Similar to the two major SSW events, the equatorial mesospheric zonal wind in 2014/15 displayed maximum westward wind with a magnitude of ~ -70 m/s along with a delay of ~ 19 days after the vortex disruption, as inferred from Table 2. In the mesospheric region, the magnitude of the peak westward wind over Kototabang is found to be nearly twice the magnitude of the peak westward wind over Esrange/Mohe. It was also noted that the peak westward over Kototabang appeared with a delay of nearly ~ 10 – 20 days after the vortex disruption, whereas the peak westward over Esrange/Mohe appeared around the time of vortex disruption. Vigorous planetary wave activity was observed during the minor SSW 2014/15 comparable to the major SSWs 2005/06 and 2008/09. The strong quasi-16-day with maximum power of $100 \text{ m}^2 \text{ s}^{-2}$ and weak 8-day was observed in the equatorial mesosphere during minor SSW 2014/15. The appearance of a quasi-16-day wave is robustly seen in all three stations Esrange, Mohe, and Kototabang with maximum intensity in the equatorial belt and weaker intensities observed in the high latitudes. Similar to the major stratospheric warming in 2005/06 and 2008/09, intrusion of planetary wave flux was seen in 2014/15 and it reached well up to the tropical latitudes. Eliassen Palm flux analysis revealed the meridional and equatorward propagation of planetary wave energy that was observed in 2014/15 similar to the major events of 2005/06 and 2008/09. In addition, the Intrusion of wave flux is more prominent in vortex split (2008/09 and 2014/15) events than in vortex displacement (2005/06). During the vortex split in 2014/15, Strong Convergence of wave forcing (negative EP flux divergence) from high latitudes were seen to propagate downward reaching up to much lower latitudes ($\sim 3^\circ \text{ N}$). This study presents the significant impact of the 2014/15 minor SSW on the high and equatorial mesosphere in comparison to the remarkable major SSWs of 2005/06 and 2008/09.

Acknowledgements & Data Availability We thank the Research Institute for Sustainable Humanosphere (RISH), Kyoto University for Kototabang Meteor Radar Observations. The distribution of this meteor radar data has been partly supported by the IUGONET (Inter-university Upper atmosphere Global Observation NETWORK) project (<http://www.iugonet.org/>) funded by the Ministry of Education, Culture, Sports, Science and Technology (MEXT), Japan. We thank the UKMO and BADC for data provision of Esrange meteor radar data (<https://data.ceda.ac.uk/badc/meteor-radars/data>) and Mohe radar data data provided by Beijing National Observatory of Space Environment, Institute of Geology and Geophysics, Chinese Academy of Sciences (<http://wdc.geophysics.ac.cn/dbList.asp?dType=MetPublish>). We also wish to thank the team behind the ECMWF ERA-Interim Reanalysis data retrieved from

the ECMWF website http://data-portal.ecmwf.int/data/d/interim_daily and the meteor radar providers of the Esrange and Mohe meteor radars.

Declarations

Conflict of Interest The authors declare that they have no conflict of interest.

References

- Andrews, D.G., McIntyre, M.E.: Planetary waves in horizontal and vertical shear: The generalized Eliassen-Palm relation and the mean zonal acceleration. *J. Atmospheric Sci.* **33**(11), 2031–2048 (1976). [https://doi.org/10.1175/1520-0469\(1976\)033%3c2031:PWIAV%3e2.0.CO;2](https://doi.org/10.1175/1520-0469(1976)033%3c2031:PWIAV%3e2.0.CO;2)
- Andrews, D. G.: Wave–mean-flow interaction in the middle atmosphere. In *Advances in geophysics* (Vol. 28, pp. 249–275). Elsevier (1985). [https://doi.org/10.1016/S0065-2687\(08\)60226-5](https://doi.org/10.1016/S0065-2687(08)60226-5)
- Andrews, D.G., Holton, J.R., Leovy, C.B.: *Middle Atmosphere Dynamics*, Vol. 40 of International Geophysics Series. Academic Press, London (1987)
- Appu, K.S.: On perturbations in the thermal structure of tropical stratosphere and mesosphere in winter. *Indian J. Radio. Space Phys.* **13**, 35–41 (1984). <http://nopr.niscpr.res.in/handle/123456789/36667>
- Bal, S., Schimanke, S., Spanghel, T., Cubasch, U.: Variable influence on the equatorial troposphere associated with SSW using ERA-Interim. *J. Earth Syst. Sci.* **126**, 1–13 (2017a). <https://doi.org/10.1007/s12040-017-0802-6>
- Bal, S., Schimanke, S., Spanghel, T., Cubasch, U.: Variable influence on the equatorial troposphere associated with SSW using ERA-Interim. *J. Earth Syst. Sci.* **126**, 1–13 (2017b)
- Baldwin, M.P., Ayarzagüena, B., Birner, T., Butchart, N., Butler, A.H., Charlton-Perez, A.J., Domeisen, D.I., Garfinkel, C.I., Garny, H., Gerber, E.P., Hegglin, M.I., Langematz, U., Pedatella, N.M.: Sudden stratospheric warmings. *Rev. Geophys.* **59**(1), e2020RG000708 (2021). <https://doi.org/10.1029/2020RG000708>
- Batubara, M., Manik, T., Suryana, R., Sitompul, P.: Early meteor echo data processing in meteor wind radar kototabang. *IEICE Techn. Rep. IEICE Tech. Rep.* **111**(239), 149–152 (2011)
- Bhagavathiammal, G.J.: Mid-winter Stratospheric Warming Effects on Tropical Convection over the Indian Sector Case Studies SSW effects on tropical convection over Indian region. *Indian J. Pure. Appl. Phys. (IJPAP)* **61**(8), 671–682 (2023). <https://doi.org/10.56042/ijpap.v61i8.1240>
- Bhagavathiammal, G.J., Sathishkumar, S., Sridharan, S., Gurubaran, S.: Comparison of the dynamical response of low latitude middle atmosphere to the major stratospheric warming events in the Northern and Southern Hemispheres. *J. Atmos. Solar Terr. Phys.* **146**, 205–214 (2016). <https://doi.org/10.1016/j.jastp.2016.06.007>
- Bhagavathiammal, G.J.: Low latitude dynamical response to vortex split sudden stratospheric warming: An Eliassen Palm Flux perspective. *Dyn. Atmos. Oceans* **91**, 101146 (2020). <https://doi.org/10.1016/j.dynatmoce.2020.101146>
- Butler, A.H., Gerber, E.P.: Optimizing the definition of a sudden stratospheric warming. *J. Clim.* **31**(6), 2337–2344 (2018). <https://doi.org/10.1175/JCLI-D-17-0648.1>
- Butler, A.H., Seidel, D.J., Hardiman, S.C., Butchart, N., Birner, T., Match, A.: Defining sudden stratospheric warmings. *Bull. Am. Meteor. Soc.* **96**(11), 1913–1928 (2015). <https://doi.org/10.1175/BAMS-D-13-00173.1>

- Butler, A.H., Sjöberg, J.P., Seidel, D.J., Rosen, K.H.: A sudden stratospheric warming compendium. *Earth Syst. Sci. Data* **9**, 63–76 (2017). <https://doi.org/10.5194/essd-9-63-2017>
- Chandran, A., Collins, R.L., Harvey, V.L.: Stratosphere-mesosphere coupling during stratospheric sudden warming events. *Adv. Space Res.* **53**(9), 1265–1289 (2014). <https://doi.org/10.1016/j.asr.2014.02.005>
- Chandran, A., Collins, R.L., Garcia, R.R., Marsh, D.R., Harvey, V.L., Yue, J., De La Torre, L.: A climatology of elevated stratopause events in the whole atmosphere community climate model. *J. Geophys. Res. Atmospheres* **118**(3), 1234–1246 (2013). <https://doi.org/10.1002/jgrd.50123>
- Charlton, A.J., Polvani, L.M.: A new look at stratospheric sudden warmings. Part I: Climatology and modeling benchmarks. *J. Climate* **20**(3), 449–469 (2007). <https://doi.org/10.1175/JCLI3996.1>
- Charlton, A.J., Polvani, L.M., Perlwitz, J., Sassi, F., Manzini, E., Shibata, K.K., Pawson, S., Nielsen, J.E., Rind, D.: A new look at stratospheric sudden warmings Part II: Evaluation of numerical model simulations. *J. Climate* **20**(3), 470–488 (2007). <https://doi.org/10.1175/JCLI3994.1>
- Chen, C., Chu, X.: Two-dimensional Morlet wavelet transform and its application to wave recognition methodology of automatically extracting two-dimensional wave packets from lidar observations in Antarctica. *J. Atmos. Solar Terr. Phys.* **162**, 28–47 (2017). <https://doi.org/10.1016/j.jastp.2016.10.016>
- Das, U., Pan, C.J., Yang, S.S.: Evolution of individual equatorial atmospheric Kelvin waves in the stratosphere from FORMOSAT-7/COSMIC-2 temperatures. *Terrestrial, Atmospheric Oceanic Sci.* **33**(1), 1–13 (2022)
- Day, K.A., Mitchell, N.J.: The 16-day wave in the Arctic and Antarctic mesosphere and lower thermosphere. *Atmos. Chem. Phys.* **10**(3), 1461–1472 (2010). <https://doi.org/10.5194/acp-10-1461-2010>
- De Wit, R.J., Hibbins, R.E., Espy, P.J., Hennem, E.A.: Coupling in the middle atmosphere related to the 2013 major sudden stratospheric warming. In: *Annales geophysicae*, vol. 33, issue 3, pp. 309–319. Copernicus GmbH, Göttingen (2015). <https://doi.org/10.5194/angeo-33-309-2015>
- Edmon, H.J., Jr., Hoskins, B.J., McIntyre, M.E.: Eliassen-Palm cross sections for the troposphere. *J. Atmospheric Sci.* **37**(12), 2600–2616 (1980). [https://doi.org/10.1175/1520-0469\(1980\)037%3c2600:EPCSFT%3e2.0.CO;2](https://doi.org/10.1175/1520-0469(1980)037%3c2600:EPCSFT%3e2.0.CO;2)
- Eliassen, A., Palm, E.: *Geophys Publ* **22**, 1 (1961)
- Eswaraiah, S., Ratnam, M.V., Kim, Y.H., Kumar, K.N., Chalapathi, G.V., Ramanajanyulu, L., Lee, J., Prasanth, P.V., Thyagarajan, K., Rao, S.V.B.: Advanced meteor radar observations of mesospheric dynamics during minor SSW over the tropical region. *Adv. Space Res.* **64**(10), (2019). <https://doi.org/10.1016/j.asr.2019.05.039>
- Eswaraiah, S., Kumar, K.N., Kim, K.H., Chalapathi, G.V., Lee, W., Jiang, G., Yan, C., Yang, G., Ratnam, M.V., Prasanth, P.V., Rao, S.V.B., Thyagarajan, K.: Low-latitude mesospheric signatures observed during the 2017 sudden stratospheric warming using the fuke meteor radar and ERA-5. *J. Atmos. Sol.-Terr.* **207**, 105352 (2020). <https://doi.org/10.1016/j.jastp.2020.105352>
- Fritz, S., Soules, S.D.: Large-scale temperature changes in the stratosphere observed from Nimbus III. *J. Atmospheric Sci.* **27**(7), 1091–1097 (1970). [https://doi.org/10.1175/1520-0469\(1970\)027%3C1091:LSTCIT%3E2.0.CO;2](https://doi.org/10.1175/1520-0469(1970)027%3C1091:LSTCIT%3E2.0.CO;2)
- Gong, Y., Wang, H., Ma, Z., Zhang, S., Zhou, Q., Huang, C., Huang, K.: A statistical analysis of the propagating quasi 16-day waves at high latitudes and their response to sudden stratospheric warmings from 2005 to 2018. *J. Geophys. Res.: Atmospheres* **124**(23), 12617–12630 (2019). <https://doi.org/10.1029/2019JD031482>
- Gu, S., Hou, X., Qi, J., TengChen, K., Dou, X.: Responses of middle atmospheric circulation to the 2009 major sudden stratospheric warming. *Earth and Planetary Physics* **4**(5), 472–478 (2020). <https://doi.org/10.26464/epp2020046>
- Harada, Y., Goto, A., Hasegawa, H., Fujikawa, N., Naoe, H., Hirooka, T.: A major stratospheric sudden warming event in January 2009. *J. Atmos. Sci.* **67**(6), 2052–2069 (2010). <https://doi.org/10.1175/2009JAS3320.1>
- Hersbach, H., Bell, B., Berrisford, P., Hirahara, S., Horányi, A., Muñoz-Sabater, J., Nicolas, J., Peubey, C., Radu, R., Schepers, D., Simmons, A.: The ERA5 global reanalysis. *Q. J. r. Meteorol. Soc.* **146**(730), 1999–2049 (2020). <https://doi.org/10.1002/qj.3803>
- Hoffmann, P., Singer, W., Keuer, D., Hocking, W.K., Kunze, M., Murayama, Y.: Latitudinal and longitudinal variability of mesospheric winds and temperatures during stratospheric warming events. *J. Atmos. Solar Terr. Phys.* **69**(17–18), 2355–2366 (2007). <https://doi.org/10.1016/j.jastp.2007.06.010>
- Hu, J., Ren, R., Xu, H., Yang, S.: Seasonal timing of stratospheric final warming associated with the intensity of stratospheric sudden warming in preceding winter. *Sci. China Earth Sci.* **58**, 615–627 (2015). <https://doi.org/10.1007/s11430-014-5008-z>
- Jia, Y., Zhang, S. D., Yi, F., Huang, C. M., Huang, K. M., Gong, Y., & Gan, Q.: Variations of Kelvin waves around the TTL region during the stratospheric sudden warming events in the Northern Hemisphere winter. In *Annales Geophysicae*, Vol. 34, No. 3, pp. 331-345. Göttingen, Germany: Copernicus Publications (2016). <https://doi.org/10.5194/angeo-34-331-2016>
- Jones, J., Webster, A.R., Hocking, W.K.: An improved interferometer design for use with meteor radars. *Radio Sci.* **33**(1), 55–65 (1998). <https://doi.org/10.1029/97RS03050>
- Kodera, K.: Influence of stratospheric sudden warming on the equatorial troposphere. *Geophysical Research Letters*, 33(6) (2006). <https://doi.org/10.1029/2005GL024510>
- Koushik, N., Kumar, K.K., Pramitha, M.: A tropical stratopause precursor for sudden stratospheric warmings. *Sci. Rep.* **12**(1), 2937 (2022)
- Koushik, N., Kumar, K.K., Siddiqui, T.A.: Westward acceleration of tropical stratopause zonal winds during major sudden stratospheric warming events. *Geophys. Res. Lett.* **47**(3), e2019GL086857 (2020). <https://doi.org/10.1029/2019GL086857>
- Koushik, N., Kumar, K.K., Ramkumar, G., Subrahmanyam, K.V., Kishore Kumar, G., Hocking, W.K., He, M., Latteck, R.: Planetary waves in the mesosphere lower thermosphere during stratospheric sudden warming: observations using a network of meteor radars from high to equatorial latitudes. *Climate Dynamics* **54**(9–10), 4059–4074 (2020)
- Koushik, N., Kumar, K.K., Ramkumar, G., Subrahmanyam, K.V.: Response of equatorial and low latitude mesosphere lower thermospheric dynamics to the northern hemispheric sudden stratospheric warming events. *J. Atmos. Solar Terr. Phys.* **169**, 66–77 (2018). <https://doi.org/10.1016/j.jastp.2018.01.021>
- Kruger, K., Naujokat, B., Labitzke, K.: The Unusual Midwinter Warming in the Southern Hemisphere Stratosphere 2002: A Comparison to Northern Hemisphere Phenomena. *J. Atmospheric Sci.* **62**(3), 603–613 (2005). <https://doi.org/10.1175/JAS-3316.1>
- Kuttippurath, J., Godin-Beekmann, S., Lefèvre, F., Nikulin, G.: Dynamics of the exceptional warming events during the Arctic winters 2003/04, 2005/06 and 2008/09. In: EGU general assembly conference abstracts, p. 5499 (2010). <https://ui.adsabs.harvard.edu/abs/2010EGUGA..12.5499K>
- Kuttippurath, J., Nikulin, G.: A comparative study of the major sudden stratospheric warmings in the Arctic winters 2003/2004–2009/2010. *Atmos. Chem. Phys.* **12**(17), 8115–8129 (2012). <https://doi.org/10.5194/acp-12-8115-2012>
- Li, N., Luan, X., Lei, J., Bolaji, O. S., Owolabi, C., Chen, J., Xu, Z., Li, G. and Ning, B.: Variations of mesospheric neutral winds and

- tides observed by a meteor radar chain over China during the 2013 sudden stratospheric warming. *J. Geophys. Res.: Space Physics*, 125(5), e2019JA027443 (2020). <https://doi.org/10.1029/2019JA027443>
- Li, Y., Kirchengast, G., Schwaerz, M., Yuan, Y.: Monitoring sudden stratospheric warmings under climate change since 1980 based on reanalysis data verified by radio occultation. *Atmos. Chem. Phys.* **23**(2), 1259–1284 (2023). <https://doi.org/10.5194/acp-23-1259-2023>
- Limpasuvan, V., Orsolini, Y.J., Chandran, A., Garcia, R.R., Smith, A.K.: On the composite response of the MLT to major sudden stratospheric warming events with elevated stratopause. *J. Geophys. Res.: Atmospheres* **121**(9), 4518–4537 (2016). <https://doi.org/10.1002/2015JD024401>
- Ma, Z., Gong, Y., Zhang, S., Zhou, Q., Huang, C., Huang, K., Yu, Y., Li, G., Ning, B., Li, C.: Responses of quasi 2 day waves in the MLT region to the 2013 SSW revealed by a meteor radar chain. *Geophys. Res. Lett.* **44**(18), 9142–9150 (2017). <https://doi.org/10.1002/2017GL074597>
- Manney, G.L., Lawrence, Z.D., Santee, S.L., Read, W.G., Livesey, N.J., Lambert, A., Froidevaux, L., Pumphrey, H.C., Schwartz, M.J.: A minor sudden stratospheric warming with a major impact: Transport and polar processing in the 2014/2015 Arctic winter. *Geophys. Res. Lett./Volume 42, Issue 18, Page: 7808–7816* (2015). <https://doi.org/10.1002/2015GL065864>
- Manney, G.L., Lawrence, Z.D.: The major stratospheric final warming in 2016: dispersal of vortex air and termination of Arctic chemical ozone loss. *Atmos. Chem. Phys.* **16**(23), 15371–15396 (2016). <https://doi.org/10.5194/acp-16-15371-2016>
- Matsuno, T.: A dynamical model of the stratospheric sudden warming. *J. Atmospheric Sci.* **28**(8), 1479–1494 (1971). [https://doi.org/10.1175/1520-0469\(1971\)028%3C1479:ADMOTS%3E2.0.CO;2](https://doi.org/10.1175/1520-0469(1971)028%3C1479:ADMOTS%3E2.0.CO;2)
- Matthias, V., Hoffmann, P., Manson, A., Meek, C., Stober, G., Brown, P., Rapp, M.: The impact of planetary waves on the latitudinal displacement of sudden stratospheric warmings. In *Annales Geophysicae* (Vol. 31, No. 8, pp. 1397–1415). Göttingen, Germany: Copernicus Publications (2013). <https://doi.org/10.5194/angeo-31-1397-2013>
- McDonald, A. J., Hibbins, R. E., & Jarvis, M. J.: Properties of the quasi 16 day wave derived from EOS MLS observations. *J. Geophys. Res.: Atmospheres*, 116(D6) (2011). <https://doi.org/10.1029/2010JD014719>
- McInturff, R. M., Ed.: Stratospheric warming: Synoptic, dynamic and general-circulation aspects. NASA Reference Publ. NASA-RP-1017, 174pp (1978)
- Medvedeva, I., Ratovsky, K.: Effects of the 2016 February minor sudden stratospheric warming on the MLT and ionosphere over Eastern Siberia. *J. Atmos. Solar Terr. Phys.* **180**, 116–125 (2018). <https://doi.org/10.1016/j.jastp.2017.09.007>
- Mitchell, N.J.: University of Bath Skymet meteor radar data collection. Centre for Environmental Data Analysis (2019). <https://catalogue.ceda.ac.uk/uuid/836daab8d626442ea9b8d0474125a446>. Accessed July 2023
- Mukherjee, B.K., Indira, K., Dani, K.K.: Perturbations in tropical middle atmosphere during winter 1984–1985. *Meteorol. Atmos. Phys.* **37**, 17–26 (1987). <https://doi.org/10.1007/BF01047007>
- Mukherjee, B.K., Ramana Murty, Bh.V.: High-level warmings over a tropical station. *Monthly Weather Review* **100** (9), 674–681 (1972). [https://doi.org/10.1175/1520-0493\(1972\)100%3C0674:HWOATS%3E2.3.CO;2](https://doi.org/10.1175/1520-0493(1972)100%3C0674:HWOATS%3E2.3.CO;2)
- Mukherjee, B.K.: Stratwrm phenomenon at low-latitudes—current status and future prospects. *Indian J. Radio Space Phys.* **19**, 193–201 (1990). <http://nopr.niscair.res.in/handle/123456789/36282>
- Mukhtarov, P., Pancheva, D., Andonov, B., Mitchell, N.J., Merzlyakov, E., Singer, W., Hocking, W., Meek, C., Manson, A., Murayama, Y.: Large-scale thermodynamics of the stratosphere and mesosphere during the major stratospheric warming in 2003/2004. *J. Atmos. Solar Terr. Phys.* **69**(17–18), 2338–2354 (2007). <https://doi.org/10.1016/j.jastp.2007.07.012>
- Nath, D., Sridharan, S., Sathishkumar, S., Gurubaran, S., & Chen, W.: Lower stratospheric gravity wave activity over Gadanki (13.5° N, 79.2° E) during the stratospheric sudden warming of 2009: Link with potential vorticity intrusion near Indian sector. *J. Atmospheric Solar-Terrestrial Phys.*, 94, 54–64 (2013). <https://doi.org/10.1016/j.jastp.2012.12.013>
- O’Neill, A.: Stratospheric sudden warmings. *Encyclopedia of Atmospheric Sciences*, J. R. Holton, J. A. Pyle, and J. A. Curry, Eds., Elsevier, 1342–1353. (2003) <https://doi.org/10.1016/B0-12-227090-8/00230-X>
- Pancheva, D., Mukhtarov, P.: Wavelet analysis on transient behaviour of tidal amplitude fluctuations observed by meteor radar in the lower thermosphere above Bulgaria. *Ann. Geophys.* **18**, 316–331 (2000). <https://doi.org/10.1007/s00585-000-0316-3>
- Pant, T., Vineeth, C., Sridharan, R.: The polar Sudden Stratospheric Warming (SSW) and its possible manifestations in the equatorial Mesosphere-Thermosphere-Ionosphere. In: 37th COSPAR Scientific Assembly, vol. 37, p. 2343 (2008). <https://ui.adsabs.harvard.edu/abs/2008cosp...37.2343P>
- Pedatella, N. M., & Harvey, V. L.: Impact of strong and weak stratospheric polar vortices on the mesosphere and lower thermosphere. *Geophysical Research Letters*, 49(10), e2022GL098877 (2022). <https://doi.org/10.1029/2022GL098877>
- Pogoreltsev, A.I., Savenkova, E.N., Pertsev, N.N.: Sudden stratospheric warmings: the role of normal atmospheric modes. *Geomag. Aeron.* **54**, 357–372 (2014). <https://doi.org/10.1134/S0016793214020169>
- Qin, Y., Gu, S.Y., Dou, X., Gong, Y., Chen, G., Zhang, S., Wu, Q.: Climatology of the quasi-6-day wave in the mesopause region and its modulations on total electron content during 2003–2017. *J. Geophys. Res. Space Physics* **124**(1), 573–583 (2019). <https://doi.org/10.1029/2018JA025981>
- Rao, R.: Wavelet Transforms. In *Encyclopedia of Imaging Science and Technology*, J.P. Hornak (Ed.) (2002). <https://doi.org/10.1002/0471443395.img112>
- Resmi, E.A., Mohanakumar, K., Appu, K.S.: Effect of polar sudden stratospheric warming on the tropical stratosphere and troposphere and its surface signatures over the Indian region. *J. Atmos. Solar Terr. Phys.* **105**, 15–29 (2013). <https://doi.org/10.1016/j.jastp.2013.07.003>
- Rhodes, C. T., Limpasuvan, V., & Orsolini, Y. J.: Eastward-propagating planetary waves prior to the January 2009 sudden stratospheric warming. *J. Geophys. Res.: Atmospheres*, 126(11), e2020JD033696 (2021). <https://doi.org/10.1029/2020JD033696>
- Sassi, F., Liu, H.L.: Westward traveling planetary wave events in the lower thermosphere during solar minimum conditions simulated by SD-WACCM-X. *J. Atmos. Solar Terr. Phys.* **119**, 11–26 (2014). <https://doi.org/10.1016/j.jastp.2014.06.009>
- Sassi, F., Garcia, R.R., Boville, B.A.: The stratopause semiannual oscillation in the NCAR Community Climate Model. *J. Atmos. Sci.* **50**(21), 3608–3624 (1993). [https://doi.org/10.1175/1520-0469\(1993\)050%3c3608:TSSOIT%3e2.0.CO;2](https://doi.org/10.1175/1520-0469(1993)050%3c3608:TSSOIT%3e2.0.CO;2)
- Sathishkumar, S., & Sridharan, S.: Planetary and gravity waves in the mesosphere and lower thermosphere region over Tirunelveli (8.7° N, 77.8° E) during stratospheric warming events. *Geophys. Res. Lett.*, 36(7) (2009). <https://doi.org/10.1029/2008GL037081>
- Sathishkumar, S., Sridharan, S., Jacobi, C.: Dynamical response of low-latitude middle atmosphere to major sudden stratospheric warming events. *J. Atmos. Solar Terr. Phys.* **71**(8–9), 857–865 (2009). <https://doi.org/10.1016/j.jastp.2009.04.002>
- Sato, Y.: Observational estimates of Eliassen and Palm flux due to quasi-stationary planetary waves. *Journal of the Meteorological*

- Society of Japan. Ser. II, 58(5), 430–435 (1980). https://doi.org/10.2151/jmsj1965.58.5_430
- Shankar Das, S., Kishore Kumar, K., Veena, S.B., Ramkumar, G.: Simultaneous observation of quasi 16-day wave in the mesospheric winds and temperature over low-latitude with SKiYMET radar. 38th COSPAR Scientific Assembly **38**, 5 (2010)
- Shepherd, M.G., Wu, D.L., Fedulina, I.N., Gurubaran, S., Russell, J.M., Mlynczak, M.G., Shepherd, G.G.: Stratospheric warming effects on the tropical mesospheric temperature field. *J. Atmos. Solar Terr. Phys.* **69**(17–18), 2309–2337 (2007). <https://doi.org/10.1016/j.jastp.2007.04.009>
- Siskind, D. E., Eckermann, S. D., McCormack, J. P., Coy, L., Hoppel, K. W., & Baker, N. L.: Case studies of the mesospheric response to recent minor, major, and extended stratospheric warmings. *J. Geophys. Res. : Atmospheres*, 115(D3) (2010). <https://doi.org/10.1029/2010JD014114>
- Siva Kumar, V., Rao, P.B., Krishnaiah, M.: Lidar measurements of stratosphere–mesosphere thermal structure at a low latitude: comparison with satellite data and models. *J. Geophys. Res.* **108**(D11), 4342 (2003). <https://doi.org/10.1029/2002JD003029>
- Sivakumar, V., Morel, B., Bencherif, H., Baray, J.L., Baldy, S., Hauchecorne, A., Rao, P. B.: Rayleigh lidar observation of a warm stratopause over a tropical site, Gadanki (13.51N, 79.21E). *Atmospheric Chem. Phys.* **4**, 1989–1996 (2004). <https://doi.org/10.5194/acp-4-1989-2004>
- Sridharan, S., Sathishkumar, S.: Observational evidence of deep convection over Indonesian sector in relation with major stratospheric warming events of 2003–04 and 2005–06. *J. Atmos. Solar Terr. Phys.* **73**(17–18), 2453–2461 (2011). <https://doi.org/10.1016/j.jastp.2011.09.007>
- Tang, Q., Zhou, C., Li, Z.S., Liu, Y. and Chen, G.Y.: Semi-Monthly Lunar Tide Oscillation of foF2 in Equatorial Ionization Anomaly (EIA) Crests During 2014–2015 SSW. *J. Geophys. Res.: Space Physics*, 126(2), p.e2020JA028708 (2021). <https://doi.org/10.1029/2020JA028708>
- Tao, M., Liu, Y., Zhang, Y.: Variation in Brewer–Dobson circulation during three sudden stratospheric major warming events in the 2000s. *Adv. Atmos. Sci.* **34**, 1415–1425 (2017). <https://doi.org/10.1007/s00376-017-6321-1>
- Torrence, C., Gilbert, P.C.: A Practical Guide to Wavelet Analysis. *Bulletin of the American Meteorological Society*. Vol. 79, Issue 1 (1998). [https://doi.org/10.1175/1520-0477\(1998\)079<0061:APGTWA>2.0.CO;2](https://doi.org/10.1175/1520-0477(1998)079<0061:APGTWA>2.0.CO;2)
- Wang, H., Akmaev, R. A., Fang, T. W., Fuller-Rowell, T. J., Wu, F., Maruyama, N., & Iredell, M. D. (2014). First forecast of a sudden stratospheric warming with a coupled whole-atmosphere/ionosphere model IDEA. *J. Geophys. Res. : Space Physics*, 119(3), 2079–2089 (2014). <https://doi.org/10.1002/2013JA019481>
- Yang, J., Xiao, C., Hu, X., Xu, Q.: Responses of zonal wind at~ 40 N to stratospheric sudden warming events in the stratosphere, mesosphere and lower thermosphere. *Sci. China Technol. Sci.* **60**, 935–945 (2017). <https://doi.org/10.1007/s11431-016-0310-8>
- Yoshida, K., Yamazaki, K.: Tropical cooling in the case of stratospheric sudden warming in January 2009: focus on the tropical tropopause layer. *Atmos. Chem. Phys.* **11**(13), 6325–6336 (2011). <https://doi.org/10.5194/acp-11-6325-2011>
- Zorkaltseva, O.S., Antokhina, O.Y., Antokhin, P.N.: Long-Term Variations in Parameters of Sudden Stratospheric Warmings According to ERA5 Reanalysis Data. *Atmospheric and Oceanic Optics* **36**(4), 370–378 (2023). <https://doi.org/10.1134/S1024856023040206>

Publisher's Note Springer Nature remains neutral with regard to jurisdictional claims in published maps and institutional affiliations.

Springer Nature or its licensor (e.g. a society or other partner) holds exclusive rights to this article under a publishing agreement with the author(s) or other rightsholder(s); author self-archiving of the accepted manuscript version of this article is solely governed by the terms of such publishing agreement and applicable law.

